Simulations of the three-dimensional Hubbard model: Half-filled band sector

J. E. Hirsch
Department of Physics, University of California, San Diego, La Jolla, California 92093
(Received 23 July 1986)

We present results of Monte Carlo simulations of the three-dimensional half-filled Hubbard model on simple-cubic 4^3 lattices and some 6^3 lattices with periodic boundary conditions, as well as of small clusters embedded in an effective medium. Magnetic properties were studied for values of the Hubbard repulsion U ranging from 0 to the bandwidth $W=12t$ (t is the hopping matrix element). Our results show that antiferromagnetism is enhanced up to $U\sim\frac{5}{6}W$ and then suppressed. The $q=0$ magnetic susceptibility is enhanced by U, although much less than predicted by the random-phase approximation. The transition temperature to an antiferromagnetic state is found to have a broad maximum around $U\sim\frac{5}{6}W$, with a maximum value of approximately $W/18$. The implications of our results for superconductivity in the attractive Hubbard model are also discussed.

I. INTRODUCTION

The magnetic properties of the Hubbard model are of interest since it is the simplest model capable of interpolating between itinerant and localized descriptions of magnetism.[1,2] The model is defined by the Hamiltonian

$$H=\sum_{\substack{i,j,\\ \sigma}} t_{ij}(c_{i\sigma}^{\dagger}c_{j\sigma}+\text{H.c.})+U\sum_i n_{i\uparrow}n_{i\downarrow}-\mu\sum_{i,\sigma} n_{i\sigma}\ . \tag{1}$$

We study here the model on a three-dimensional simple-cubic lattice with nearest-neighbor hopping only t, in the half-filled band sector ($\mu=U/2$, one electron per site). In this sector the model is expected to be an antiferromagnetic insulator for all values of U, and has been widely used to describe the transition-metal monoxides MnO, FeO, CoO, and NiO.[3] These materials are electrically insulating and undergo a transition to an antiferromagnetic state as the temperature is lowered.

For large U, the dominant interaction in the Hamiltonian Eq. (1) is Anderson superexchange, and one has an effective antiferromagnetic Heisenberg Hamiltonian

$$H_{\text{eff}}=\sum_{\langle i,j\rangle}\frac{t_{ij}^2}{U}\boldsymbol{\sigma}_i\cdot\boldsymbol{\sigma}_j \tag{2}$$

describing the magnetic degrees of freedom. The effective exchange $J_{\text{eff}}=t^2/U$, and hence the transition temperature to a magnetic state, are decreasing functions of U. The Hamiltonian Eq. (2) correctly describes the magnetic degrees of freedom to lowest order in t/U. From high-temperature series estimates for the transition temperature in the antiferromagnetic $S=\frac{1}{2}$ Heisenberg model[4] one has for the Hubbard model for large U

$$T_c\cong 3.83t^2/U\ . \tag{3}$$

For small U, summation of the ladder graphs for the magnetic susceptibility [random-phase approximation (RPA)] yields

$$\chi=\frac{\chi_0}{1-\dfrac{U\chi_0}{2}} \tag{4}$$

with χ_0 the susceptibility for the noninteracting case. Although Eq. (4) is rigorously valid only to lowest order in U/t, it is sometimes used even for large values of U/t. From Eq. (4) one obtains a criterion for the transition to a magnetic state,

$$1=\frac{U\chi_0(q)}{2} \tag{5}$$

(Stoner criterion). Equation (5) yields a transition temperature T_c which is an increasing function of U. For the present case the magnetic susceptibility for the noninteracting case $\chi_0(q)$ peaks at $q=\pi$ and actually diverges as $T\to 0$ due to nesting of the Fermi surface. Hence, Eq. (5) predicts a transition to an antiferromagnetic state for any nonzero value of U, at a critical temperature T_c that is a rapidly increasing function of U, asymptotically given by the BCS form,

$$kT_c=1.13\frac{W}{2}e^{-1/\rho(0)U} \tag{6}$$

with $W=12t$ the bandwidth and $\rho(0)$ the density of states at the Fermi energy. The RPA approximation is equivalent to a Hartree-Fock self-consistent decoupling of the interaction term in Eq. (1).

The purpose of this paper is to interpolate between the weak- and strong-coupling analytic solutions [Eqs. (6) and (3)] by means of Monte Carlo simulations. We study magnetic properties on small lattices for U up to $12t$ essentially with no approximations. In Sec. II we describe the methodology used, and in Sec. III we present results for various magnetic properties for 4^3 and some 6^3 lattices as functions of U and temperature. Because we can only treat small lattices, it is difficult to extract a transition temperature from simulations with the usual periodic boundary conditions. For this reason, we apply in Sec. IV a self-consistent-boundary-field approach[5] where we study

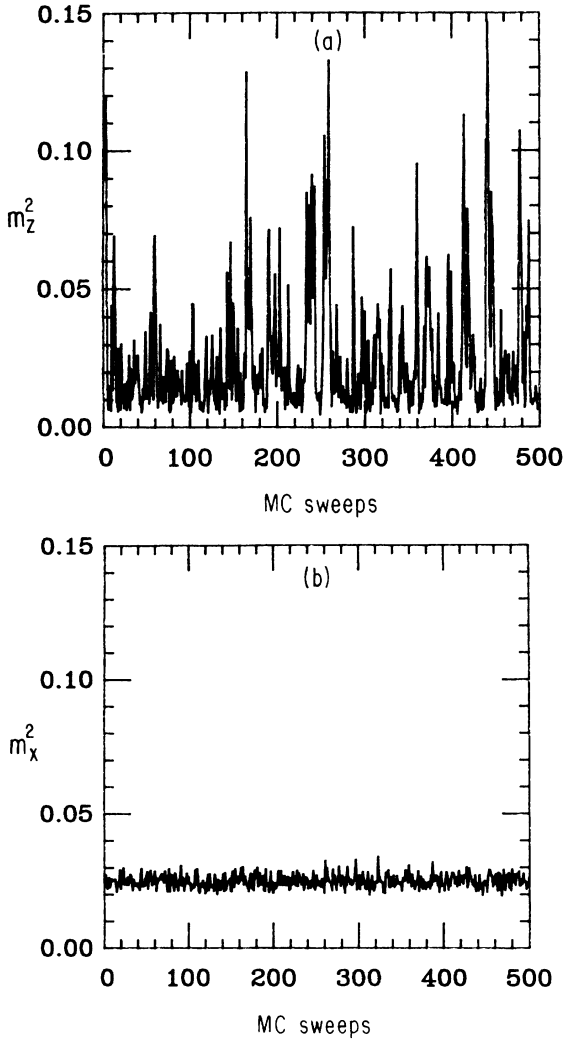

FIG. 1. Staggered magnetization squared in the z direction (a) and in the xy plane (b) vs Monte Carlo sweeps, $U=6$, $\beta=1.33$, 4^3 lattice. The averages are the same but the variance is much larger in (a).

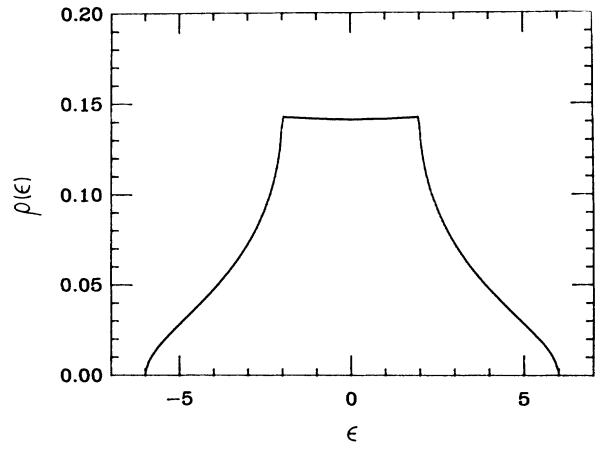

FIG. 2. Density of states of three-dimensional simple cubic lattice.

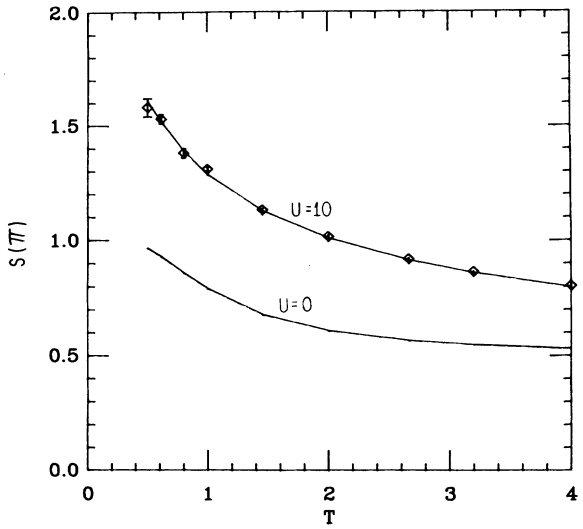

FIG. 3. Magnetic structure factor vs temperature for a two-site lattice. The diamonds are the Monte Carlo results for $U=10$, the full lines are exact results for $U=10$ and 0 (the algorithm gives exact results for $U=0$).

properties of a small cluster embedded in an effective medium. This approach has been shown to give accurate answers for classical spin systems.[5] We obtain the critical temperature T_c versus U for up to $U=12t$. In Sec. V we discuss the implications of our results for superconductivity in the attractive Hubbard model. Finally, we summarize our conclusions in Sec. VI.

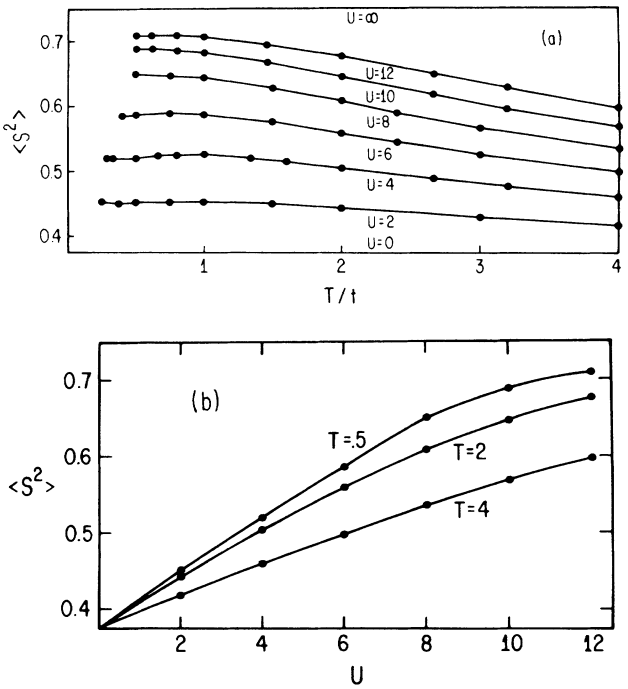

FIG. 4. Local magnetic moment vs (a) temperature (4^3 lattice) and (b) U. The error in the Monte Carlo data is smaller than the points.

II. METHODOLOGY

The approach used has been discussed in detail elsewhere,[6,7] so that we only summarize the essential points here for completeness. The partition function is written as

$$Z = \mathrm{Tr} e^{-\beta H} = \mathrm{Tr} \prod_{l=1}^{L} e^{-\Delta\tau H} \cong \mathrm{Tr} \prod_{l=1}^{L} e^{-\Delta\tau H_0} e^{-\Delta\tau H_1} \quad (7)$$

with an error $O(\Delta\tau^2 tU)$ in the breakup in Eq. (1). The electron-electron interaction is eliminated through a discrete Hubbard-Stratonovich transformation,

$$e^{-\Delta\tau U[n_\uparrow n_\downarrow - \frac{1}{2}(n_\uparrow + n_\downarrow)]} = \tfrac{1}{2}\mathrm{Tr}_\sigma e^{\lambda\sigma(n_\uparrow - n_\downarrow)} \quad (8)$$

and the trace over fermion degrees of freedom in Eq. (7) is performed. The result is

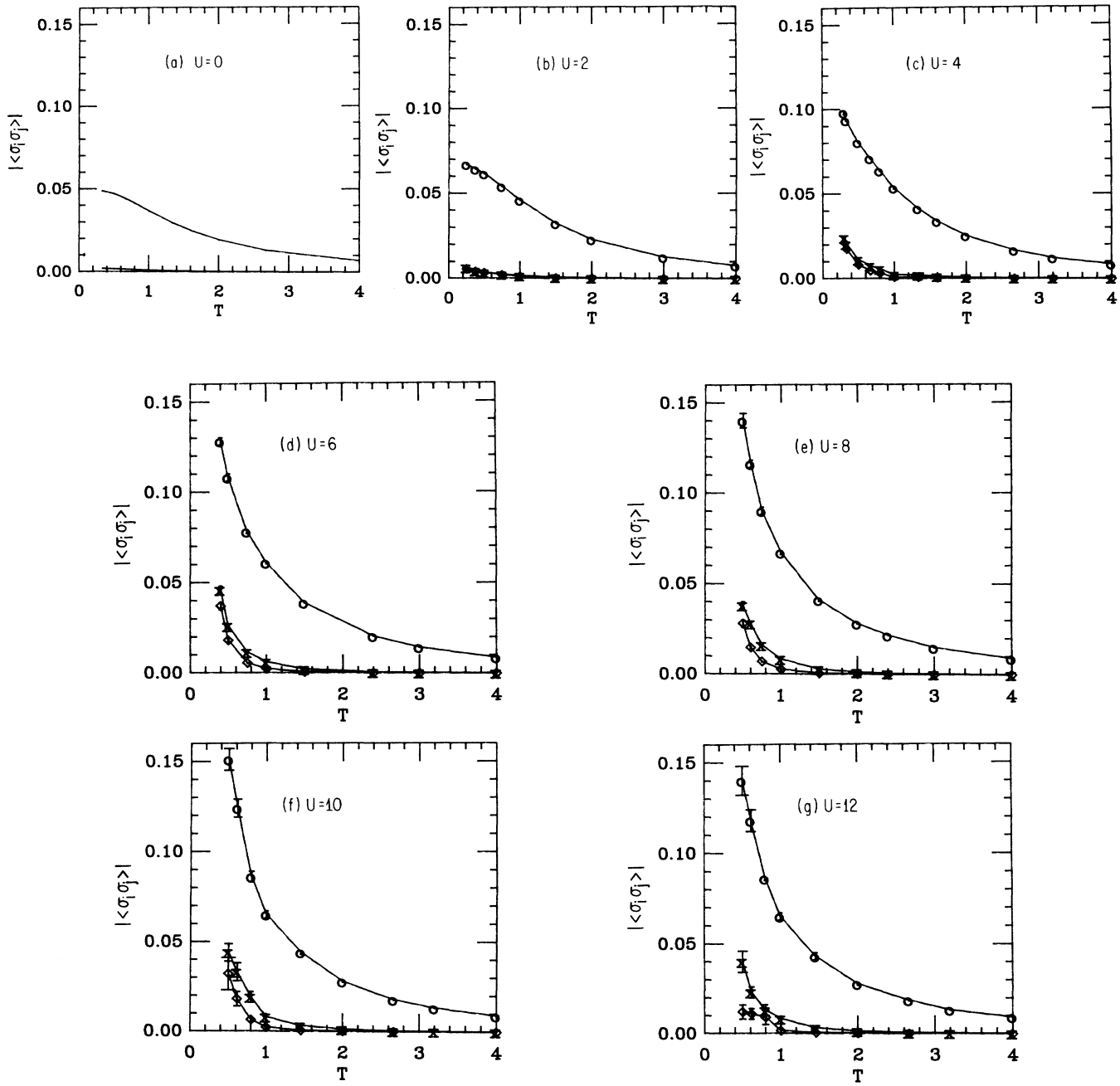

FIG. 5. Spin-spin correlation functions (absolute value) vs temperature. The circles, crosses, and diamonds correspond to nearest neighbor (NN), next-nearest neighbor (NNN) and third-nearest neighbor (3NN), respectively. The NN and 3NN correlations are always negative.

$$Z = \mathrm{Tr}_{\{\sigma_i(l)\}} \det\left[1+\prod_{l=1}^{L} e^{-\Delta\tau K} e^{V^{+}(l)}\right] \times \det\left[1+\prod_{l=1}^{L} e^{-\Delta\tau K} e^{V^{-}(l)}\right], \quad (9)$$

where t is an $N\times N$ matrix, $(t)_{ij}=t_{ij}$, and $V^{\mu}(l)$ is a diagonal $N\times N$ matrix,

$$V^{\mu}_{ij}(l)=\delta_{ij}\lambda\mu\sigma_i(l) . \quad (10)$$

Due to particle-hole symmetry there is a relation between the two determinants in Eq. (9) so that the product is positive definite for all configurations,[7] and we can formally write

$$Z=\mathrm{Tr}_{\{\sigma_i(l)\}} e^{-H_{\mathrm{eff}}\{\sigma\}} , \quad (11)$$

where H_{eff} is a nonlocal Hamiltonian describing the interactions between the Ising spins on a four-dimensional lattice. Physically, the Ising variables represent the z component of the electron spin at each site, since the following relation holds:

$$\langle [n_{i\uparrow}(\tau)-n_{i\downarrow}(\tau)][n_{j\uparrow}(0)-n_{j\downarrow}(0)]\rangle = \frac{1}{1-e^{-\Delta\tau U}}\langle \sigma_i(\tau)\sigma_j(0)\rangle , \quad (12)$$

relating correlation functions of the Ising and fermion spins. The charge degrees of freedom have been integrated out of the problem in arriving at Eq. (11), and this is the reason for the resulting weights being always positive. In fact, a more general transformation than Eq. (8) can be found that keeps part of the charge degrees of freedom, but in that case negative weights do occur.[8]

We use an exact updating procedure to do the Monte Carlo simulation,[6] and measure equal time and zero-frequency spin and charge correlations. For example, the spin-spin correlations measured in the z and in the x direction are

$$C^{z}_{ij}=\langle (n_{i\uparrow}-n_{i\downarrow})(n_{j\uparrow}-n_{j\downarrow})\rangle , \quad (13a)$$

$$C^{x}_{ij}=\langle (c^{\dagger}_{i\uparrow}c_{i\downarrow}+c^{\dagger}_{i\downarrow}c_{i\uparrow})(c^{\dagger}_{j\uparrow}c_{j\downarrow}+c^{\dagger}_{j\downarrow}c_{j\uparrow})\rangle . \quad (13b)$$

Although Eqs. (13a) and (13b) should agree for the averages because of the spin-rotational invariance of the system, their variance turns out to be very different. As an example, Fig. 1 shows the staggered magnetization measured in the z direction and in the x direction for one case. It can be seen that the fluctuations for the latter are significantly smaller. This was found to be the case to varying degrees for all spin-dependent quantities in all cases studied.

III. NUMERICAL RESULTS

Figure 2 shows the density of states for the three-dimensional simple cubic lattice. The band extends from -6 to 6 (in units where $t=1$), and in this paper we con-

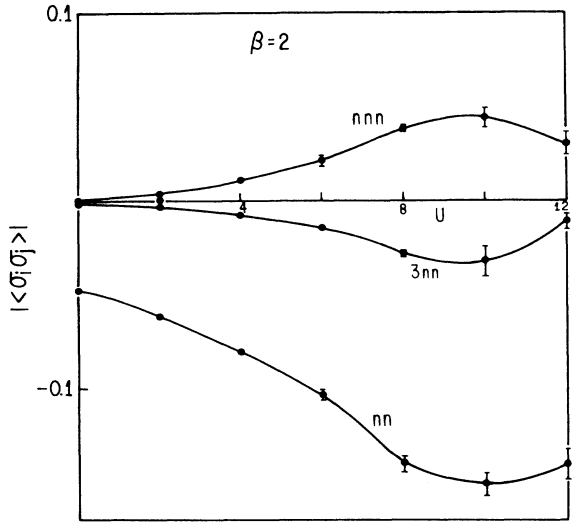

FIG. 6. Spin-spin correlation functions vs U for $\beta=2$.

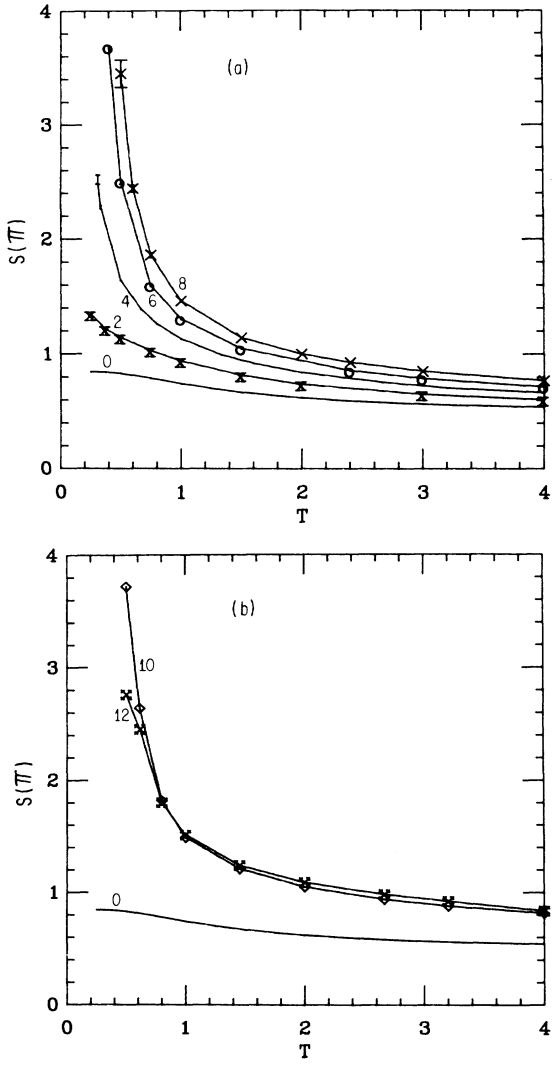

FIG. 7. Magnetic structure factor at $\mathbf{q}=\pi$ vs temperature. The numbers next to the curves indicate the value of U.

sider the half-filled-band case ($\mu = U/2$). We have studied the system for U ranging from 0 to 12.

The Monte Carlo procedure used here has already been tested extensively elsewhere.[7,9] We have used a time slice size $\Delta\tau\sqrt{tU} = 0.25$, for which the systematic error due to the breakup should be smaller than the statistical error. As an example, Fig. 3 shows the magnetic-structure factor $S(q=\pi)$ for $U=10$ on a two-site lattice, compared with exact diagonalization results. Typical Monte Carlo runs were 200 warmup sweeps, and 1000–2000 measurements, with one to two sweeps through the lattice between measurements. The statistical error is smaller than the points where not shown.

Figure 4(a) shows the local magnetic moment,

$$\langle S^2 \rangle = \tfrac{3}{4}\langle (n_{i\uparrow} - n_{i\downarrow})^2 \rangle \tag{14}$$

versus temperature for various U. It increases slowly as the temperature decreases and levels off at low T. Figure 4(b) shows the U dependence for various temperatures. The results for $T=0.5$ should be very close to the ground-state values. For $U=12$ (bandwidth) the local moment at low T is quite close to its $U=\infty$ value (perfectly localized spins). The behavior versus temperature is smooth, and similar to the two- and one-dimensional cases.[7] In units of the bandwidth the Hubbard interaction is more effective in localizing the electrons as the dimensionality increases.

Figure 5 shows spin-spin correlation functions versus temperature for U up to 12. The spin-spin correlations beyond nearest neighbor only start to build up below $T=1$. For the lowest temperature studied the maximum value attained by the nearest-neighbor spin correlation is still quite small. As U is increased beyond 10 the correlations actually start to decrease. This is clearly shown in Fig. 6, where we plot the spin-spin correlations versus U for $T=0.5$. Clearly, as U becomes stronger the antiferromagnetic coupling $J=t^2/U$ is decreasing and thus the correlations at a fixed temperature will decrease. One may interpret the value $U \sim 10t$ as the crossover value between band magnetism and localized magnetism.

Figure 7 shows the magnetic-structure factor

$$S(q) = \frac{1}{N}\sum_{i,j} e^{iq(R_i - R_j)} \langle \sigma_x^i \sigma_x^j \rangle \tag{15}$$

for $\mathbf{q}=(\pi,\pi,\pi)$ and U from 0 to 12. $S(\pi)$ starts to increase rapidly below $T=1$, indicating that the system is developing long-range order. Again, the strongest correlations occur for $U \sim 10$.

A similar behavior is observed in the magnetic susceptibility,

$$\chi(q) = \frac{1}{N}\sum_{i,j} e^{iq(R_i - R_j)} \int_0^\beta d\tau \langle \sigma_x^i(\tau)\sigma_x^j(0) \rangle \tag{16}$$

at $q=\pi$. Figure 8 shows the results for U up to 8 only, the susceptibility increasing sharply at low temperatures. For larger values of U (not shown) $\chi(\pi)$ levels off and

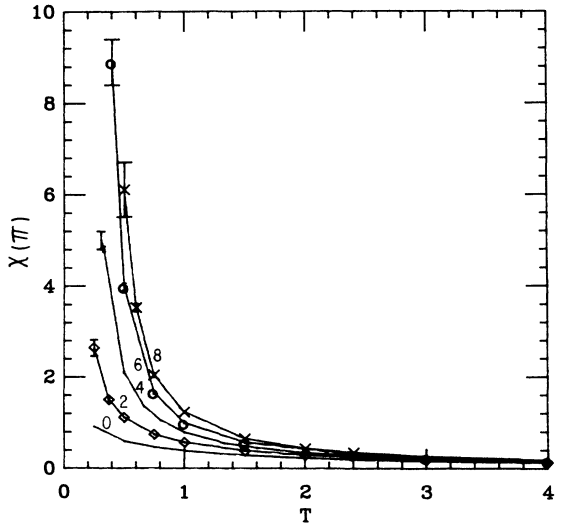

FIG. 8. Magnetic susceptibility at $\mathbf{q}=\pi$ vs temperature.

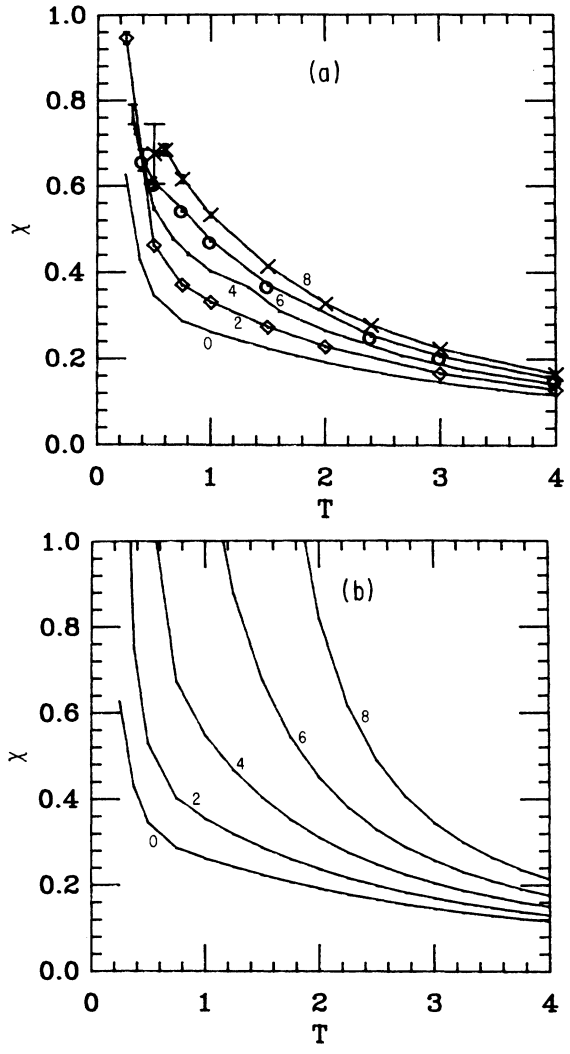

FIG. 9. Magnetic susceptibility at $\mathbf{q}=0$ vs temperature for $U=0,2,4,6,8$. (a) Monte Carlo results, (b) RPA predictions.

starts to decrease slowly at $U=12$.

It is also interesting to examine the susceptibility at $q=0$, shown in Fig. 9. It can be seen that it also is enhanced by the Hubbard interaction, although much less than the $q=\pi$ susceptibility. The enhancement is also quite small compared to the RPA prediction [Fig. 9(b)],

$$\chi(q)=\frac{\chi_0(q)}{1-\frac{U}{2}\chi_0(q)} . \tag{17}$$

Although it is expected that RPA overestimates the enhancement, Fig. 9 provides quantitative information about how good the RPA is. It is grossly in error at low temperatures for all cases except $U=2$.

In order to determine the point where the system undergoes a phase transition, it is necessary to study different size lattices. Figure 10 shows $S(\pi)$ and $\chi(\pi)$ for $U=8$ on 2^3, 4^3, and 6^3 lattices (in order that the 2^3 results agree with the larger lattices for high temperature, one has to take $t=1/\sqrt{2}$ in that case). It can be seen that the system is starting to develop long-range order at low T since the correlations diverge more rapidly on the larger lattices. Unfortunately, it is not possible to obtain reliable answers for T_c from simulations on such small lattices. For that reason we turn in Sec. IV to a self-consistent-field determination of T_c.

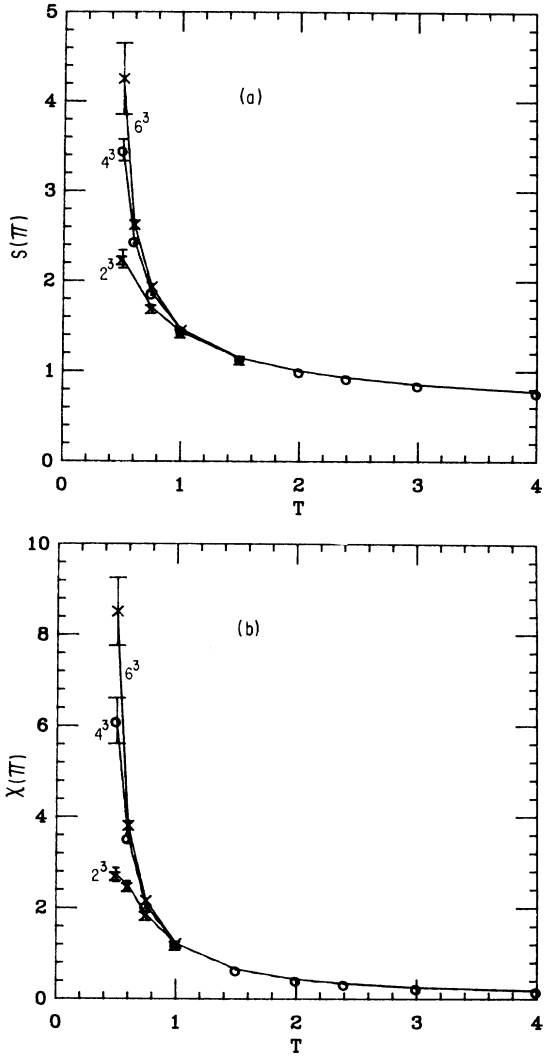

FIG. 10. (a) $S(\pi)$ and (b) $\chi(\pi)$ vs temperature for $U=8$ and lattice sizes 2^3, 4^3, and 6^3.

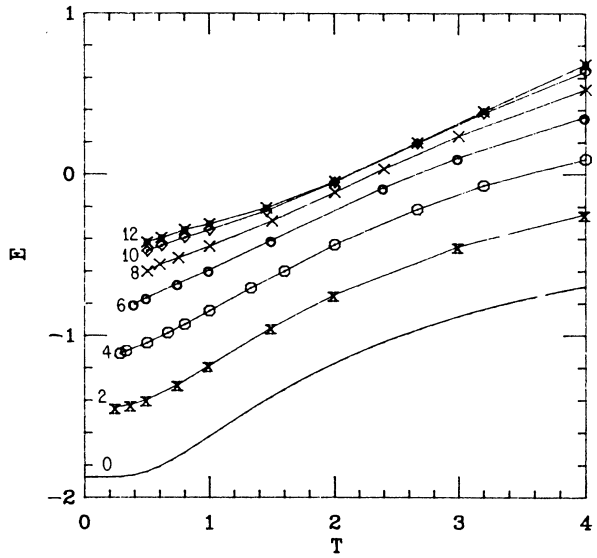

FIG. 11. Energy vs temperature for $U=0$ to 12, 4^3 lattice.

To conclude this section we show in Fig. 11 the energy as a function of temperature for several values of U. From taking the numerical derivative one can obtain the

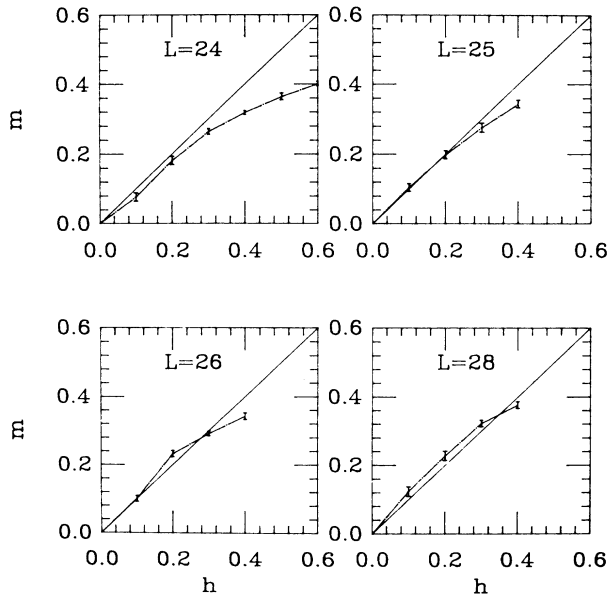

FIG. 12. Magnetization vs staggered field at the boundary for a 3^3-site cluster embedded in a 4^3-site lattice, $U=4$, $\Delta\tau=0.125$. A self-consistent non-zero solution is obtained for $L\geq 25$, i.e., $\beta\geq 3.125$.

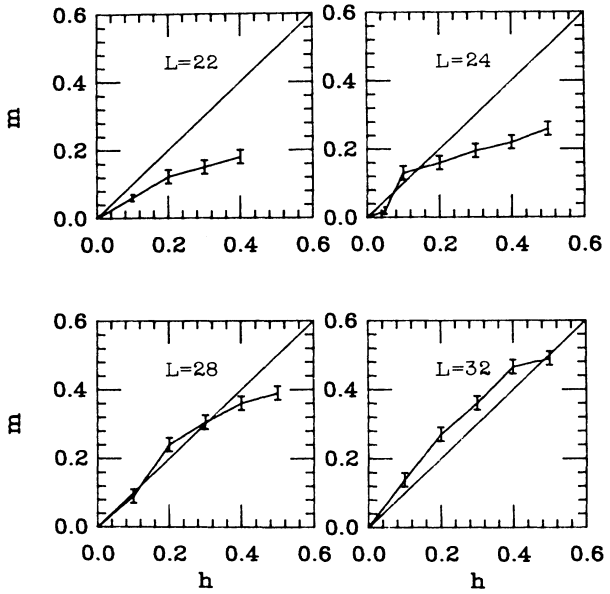

FIG. 13. Same as Fig. 12 for $U=8$, $\Delta\tau=0.0625$.

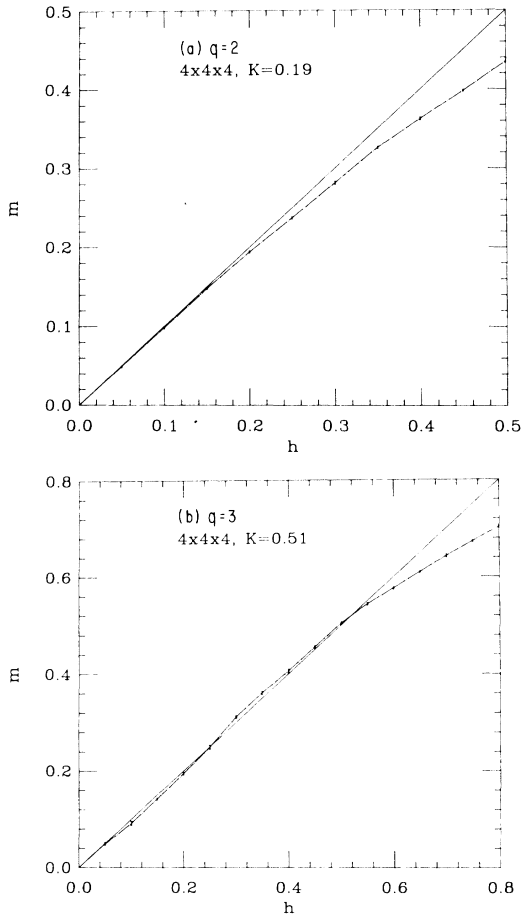

FIG. 14. Magnetization vs boundary field at the critical temperature for (a) Ising model and (b) three-state Potts model, for the same lattice sizes as Figs. 12 and 13.

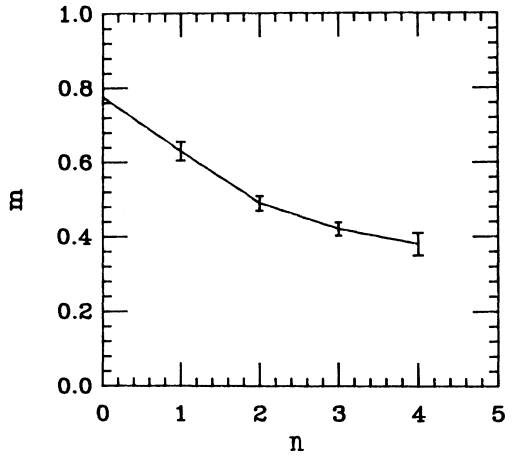

FIG. 15. Magnetization vs cluster size for $U=6$, $T=0.43$.

specific heat. In order to study the detailed form of the specific-heat curves one needs, however, more closely spaced points and higher statistics than we have used so far.

IV. SELF-CONSISTENT-FIELD BOUNDARY CONDITIONS

In this section we discuss an approach which, although approximate, yields a sharp critical temperature T_c. The method was introduced by Binder[5] in his study of the classical Heisenberg ferromagnet, where it yielded results in close agreement with high-temperature series expansions even for rather small lattices.

We consider a small cluster of atoms embedded in an effective medium. Inside the cluster we decouple the interaction by introducing Ising variables as in Eq. (8) over which we will trace using the Monte Carlo method. Outside the cluster we decouple the interaction by introducing an effective frozen staggered field,

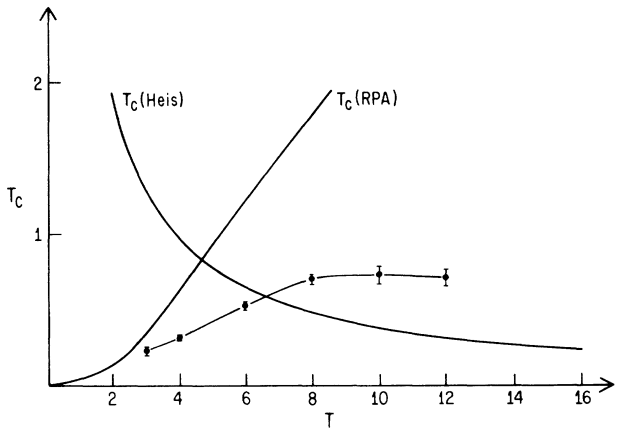

FIG. 16. Critical temperature for the paramagnetic-antiferromagnetic transition vs U. The RPA weak-coupling and Heisenberg strong-coupling predictions are obtained from Eqs. (3) and (5), respectively.

$$e^{-\Delta\tau U[n_{i\uparrow}n_{i\downarrow}-(n_{i\uparrow}+n_{i\downarrow})]/2}\cong e^{h_i(n_{i\uparrow}-n_{i\downarrow})} \tag{18}$$

with

$$h_i=\Delta\tau U\langle n_{i\alpha}\rangle(-1)^{\alpha}=(-1)^i h \tag{19}$$

and the mean field h_i is determined by the self-consistent condition Eq. (19), where $\langle n_{i\alpha}\rangle$ is the magnetization inside the cluster.

Figures 12 and 13 show results for the staggered magnetization

$$m=\sum_i(-1)^i\langle n_{i\uparrow}-n_{i\downarrow}\rangle \tag{20}$$

in a 3^3-site cluster embedded in a 4^3 lattice versus the boundary field h for $U=4$ and 8. As T is lowered, a self-consistent solution is obtained at a critical temperature T_c. Note that particularly for the larger value of U the curve is S shaped, which is indicative of a first-order transition.

As a check on the effective field boundary condition method, we have applied it to the three-dimensional q-state Potts model[10] using the same size clusters as in the Hubbard simulation. Figure 14 shows the results for the Ising case ($q=2$) and the $q=3$ case. It can be seen that the method correctly predicts a first-order transition for $q=3$ and a continuous one for $q=2$. The values of T_c obtained in this case are roughly 15% larger than the exact ones.

As an example of the dependence of our results on the size of the cluster used, Fig. 15 shows the self-consistent magnetization versus cluster size. The size dependence does seem to be small around cluster size 3, which is where we extracted our results for T_c from. We estimate that our results could overestimate T_c up to 20%.

Figure 16 shows the results for the critical temperature obtained in this fashion as a function of U. The RPA calculation gives a rapidly increasing T_c with U; for large U we plot the predictions of high-temperature expansions for the $S=\frac{1}{2}$ Heisenberg model,[4] Eq. (3). The Monte Carlo results show that T_c peaks around $U\sim 10$, in accordance with the results for the spin-spin correlation functions, and that the maximum value of T_c is roughly $\frac{1}{18}$ of the bandwidth. An interesting feature of Fig. 16 is that the values of T_c for the Hubbard model at large U are well above the Heisenberg-model predictions. Although the Monte Carlo results probably overestimate T_c somewhat, it appears that the effect is real. This implies that when U is reduced from infinity and charge fluctuations are allowed magnetism is actually enhanced, contrary to what one might have expected. Another interesting feature of our results is that the transition appears to be first order for intermediate values of U. Clearly, this needs to be further investigated.

V. THE ATTRACTIVE HUBBARD MODEL

The results discussed in Sec. IV are relevant to the properties of the attractive Hubbard model in the half-filled band sector, since, as is well known, a particle-hole transformation maps $U>0$ into $U<0$. The transformation is[11]

$$\begin{aligned} d_{i\uparrow}&=c_{i\uparrow}\ ,\\ d_{i\downarrow}&=c_{i\downarrow}^{\dagger}(-1)^i\ , \end{aligned} \tag{21}$$

and only works rigorously on bipartite lattices like the one considered here. Under this transformation, spin correlations in the xy plane are mapped onto superconducting (pairing) correlations, since

$$\sigma_x^i=c_{i\uparrow}^{\dagger}c_{i\downarrow}+c_{i\downarrow}^{\dagger}c_{i\uparrow}\rightarrow d_{i\uparrow}^{\dagger}d_{i\downarrow}^{\dagger}+d_{i\downarrow}d_{i\uparrow} \tag{22}$$

so that the existence of long-range magnetic order in the repulsive case corresponds to superconducting long-range order in the attractive case. For weak coupling, the Stoner condition for antiferromagnetism Eq. (5) translates into the BCS equation; for strong coupling, the transition in the antiferromagnetic model corresponds to a "bipolaronic" superconducting transition,[12] where pairs tightly coupled in real space undergo Bose condensation. Our results then connect smoothly these two regimes, and imply that the maximum superconducting temperature for the three-dimensional (3D) attractive Hubbard model is $T_c\sim W/18$.

It will be of interest to extend these results to other than half-filled-band cases, where the equivalence between attractive and repulsive cases no longer holds. The half-filled-band case is very special in that one has coexistence of superconducting and charge-density-wave long-range order (corresponding to magnetic order in the xy plane and in the z directions). This degeneracy is removed in the non-half-filled-band cases, which will exhibit superconducting long-range order only, although setting in at a lower temperature than the case discussed here.

VI. CONCLUSIONS

We have discussed results of Monte Carlo simulations of the half-filled Hubbard model on a three-dimensional simple cubic lattice. Our main findings can be summarized as follows.

(1) The model always exhibits antiferromagnetic correlations. The magnetic correlations increase with U until $U\sim 10$ (~ 0.85 of the bandwidth), and then start to decrease. Thus, $U\sim 85W$ can be interpreted as the point where the system crosses over from "itinerant magnetism" to "localized magnetism."

(2) The transition temperature to an antiferromagnetic state increases slowly with U until it levels off around $U\sim 10$, and starts to decrease for $U\sim 12t$ (bandwidth). The maximum transition temperature is around (and probably somewhat smaller than) $T_c^{\max}\sim W/18$.

(3) When coming down from $U=\infty$, the transition temperature increases first beyond the Heisenberg model predictions (lowest order in t/U), i.e., charge fluctuations enhance magnetism.

(4) The transition appears to be first order for intermediate values of U.

(5) RPA greatly overestimates the enhancement of the magnetic susceptibility with the interaction for all $U\geq 0.1W$.

(6) Our results for the repulsive Hubbard model apply, suitably reformulated, to the attractive case. Recently,

Nozieres and Schmitt-Rink[13] studied the connection between weak- and strong-coupling superconductivity in the attractive Hubbard model, and concluded that the transition temperature is a continuous function of U, but were unable to estimate the maximum transition temperature analytically. Our results confirm their picture and give an estimate (certainly at least an upper bound) for the maximum superconducting transition temperature for the half-filled case, as well as the value of U for which it occurs.

In summary, we believe this study has established some of the features of the three-dimensional half-filled Hubbard model, and it raised some questions that should be further clarified by simulations on larger lattices and at lower temperatures. It should also be of interest to study properties of the model in other than half-filled-band cases, and work in that direction is in progress.

ACKNOWLEDGMENTS

This work was supported by the National Science Foundation under Grant No. DMR-82-17881 and DMR-85-17756. Computations were performed using the Cray 1S at the University of Minnesota, supported by the OASC at NSF. The author is grateful to the A. P. Sloan Foundation, Cray Research, and Exxon Corporation for financial support, and to H. Shiba for pointing out an error in the original version of the manuscript.

[1]J. Hubbard, Proc. R. Soc. London, Ser. A **276**, 283 (1963); **281**, 401 (1964).

[2]*Electron Correlation and Magnetism in Narrow-Band Systems*, edited by T. Moriya (Springer, New York, 1981).

[3]See, for example, B. H. Brandow, Adv. Phys. **26**, 651 (1977) and references therein.

[4]G. S. Rushbrooke, G. A. Baker, Jr., and P. J. Wood, in *Phase Transitions and critical Phenomena*, edited by C. Domb and M. S. Green (Academic, New York, 19xx), p. 245.

[5]K. Binder, Phys. Lett. A **30**, 273 (1969); H. Müller-Krumbhaar and K. Binder, Z. Phys. **254**, 269 (1972).

[6]R. Blankenbecler, D. J. Scalapino, and R. L. Sugar, Phys. Rev. D **24**, 2278 (1981); D. J. Scalapino and R. L. Sugar, Phys. Rev. B **24**, 4295 (1981).

[7]J. E. Hirsch, Phys. Rev. B **31**, 4403 (1985).

[8]J. E. Hirsch, Phys. Rev. B **34**, 3216 (1986).

[9]J. E. Hirsch, Phys. Rev. B **28**, 4059 (1983).

[10]F. Y. Wu, Rev. Mod. Phys. **54**, 235 (1982).

[11]V. J. Emery, Phys. Rev. B **14**, 2989 (1976).

[12]A. Alexandrov and J. Ranninger, Phys. Rev. B **24**, 1164 (1981).

[13]P. Nozieres and S. Schmitt-Rink, J. Low Temp. Phys. **39**, 195 (1985).